Article

Mean Zonal Drift Velocities of Plasma Bubbles estimated from Keograms of Nightglow All-Sky Images from the Brazilian Sector

Fabio Vargas [1]*, Christiano Brum [2], Pedrina Terra [2] and Delano Gobbi [3]

1 University of Illinois at Urbana-Champaign, USA; fvargas@illinois.edu
2 University of Central Florida/Arecibo Observatory, USA; christiano.brum@ucf.edu (C.B.); pedrina.santos@ucf.edu (P.T.)
3 National Institute for Space Research, Brazil; delano.gobbi@inpe.br
* Correspondence: fvargas@illinois.edu
† Current address: 306 N. Wright St., 5066 ECEB, MC-702, Urbana, Illinois, USA, 61801

Abstract: We present in this work a method for estimation of plasma bubble mean zonal drift velocities using keograms generated from images of the OI 6300.0 nm nightglow emission collected from an equatorial station – Cariri (7.4°S, 36.5°W), and a mid-latitude station – Cachoeira Paulista (22.7°S, 45°W), both in the Brazilian sector. The mean zonal drift velocities were estimated for 239 events recorded from 2000 to 2003 in Cariri, and for 56 events recorded over Cachoeira Paulista from 1998 to 2000. It was found that plasma bubble zonal drift velocities are smaller ($\sim$60 ms^{-1}) for events occurring later in the night compared to those occurring earlier ($\sim$150 ms^{-1}). The decreasing rate of the zonal drift velocity is of $\sim$10 ms^{-1}/h. We have also found that, in general, bubble events appearing first in the west-most region of the keogram are faster than those appearing first in the east-most region of the keograms. Larger zonal drift velocities occur from 19 LT to 23 LT in a longitude range from 37° to 33°. The method of velocity estimation using keograms compares favorably against the mosaic method developed by [1], but the standard deviation of the residuals for the zonal drift velocities from the two methods is $\sim$15 ms^{-1}

Keywords: all-sky imager; ionospheric plasma bubble; zonal drift velocity; keograms; nightglow; OI6300 thermospheric emission

1. Introduction

Ionospheric plasma bubbles are extensive spatial regions of accentuated reduction of ions along the magnetic field lines. In the plasma bubble region, the electron density is rarefied due instability processes appearing in the equatorial, low latitude area. The first observations of ionospheric plasma bubbles in the Brazilian sector were reported by Sobral et al. (1980a, b) using scanning photometers. Since then, this phenomena has been extensively studied using radar [2–5] and optical techniques [1,6–13].

Studies revealed that ionospheric plasma bubbles generally have strong correlation with the Spread F phenomena, with maximal occurrence rate in summer months, whereas in winter times only few bubble occurrences have been recorded [9]. It was also noticed that the plasma bubbles are correlated with solar activity. For instance, [14] reported an increasing of 80% in their occurrence rate during solar maximum. The dynamics of these plasma bubbles includes the unwell-known seeding process after the sunset in equatorial latitudes following the upward-going movement and spreading of the plasma to low latitudes towards magnetic conjugate points along the geomagnetic field lines. This phenomena has deep effects in the atmospheric region lying among 80 to 300 km of altitude,

Peer-reviewed version available at Atmosphere 2020, 11, 69; doi:10.3390/atmos11010069

mainly in radio communication and GPS positioning throughout the equatorial region. The processes of seeding by gravity waves and growth of the Rayleigh-Taylor instability, responsible by bubble's vertical development, are not well understood yet [15,16].

Ionospheric plasma bubbles usually present relatively large velocities towards the east and its spatial structure exhibit considerable time evolution. These zonal drifts result from the vertical polarization electric fields, which are generated through complex interactions among the tidal winds, the geomagnetic field and the ionospheric plasma in the F region. Consequently, plasma bubbles are strongly aligned with the geomagnetic equator field lines, and their zonal drift velocities show large variability. [13] found that these velocities vary according to the month, decrease with the local time, and peak before local midnight. They also observed an increase of these velocities with the solar activity.

The subject of the present study is to determine the mean and instantaneous zonal drift velocities of plasma bubbles events recorded in OI6300 nightglow image data and keograms. We have carried out a comparison of our keogram method for zonal drift velocities derivation with a another named mosaic method. In Section 2 we present the instrumentation, the database, and the methodology used to estimate zonal drift velocities of the plasma bubble from keograms. Section 3 presents the results of the analysis and discusses our findings. Finally, Section 4 gives the main conclusions according to the discussion of the results.

2. Data and Methodology

with all-sky CCD imagers operating at the low latitude station named Cachoeira Paulista (22.7°S, 45°W) (hereafter CP), and at the equatorial station named Cariri (7.4°S, 36.5°W) (hereafter CA), both in the Brazilian territory. A full discussion of how the redline is generated in the nighttime thermosphere can be found in [17] and references therein. A detailed description of the instruments used during the observation periods is given by [18]. In CA, were observed 106 nights with the occurrence of plasma plasma bubbles from 2000 to 2003, and 239 structures were identified using keograms built from the airglow images. For the CP station, it were observed 56 plasma bubble events from 1998 to 2000. Based on these records, it was possible to estimate the zonal drift velocities of these bubbles using west-east keogram images.

2.1. Keograms

Frequently, a plasma bubble footprint appears in OI6300 airglow images and can be noticed as sporadic dark regions in the images. They are associated with ion density rarefaction in the ionosphere around ∼250-300 km of altitude for this specific wavelength emission. The keogram method used in this work summarizes the plasma bubble behavior obtained from images along an entire night.

The word keogram comes from keoitt, an ancient Eskimo word that means boreal aurora. In the beginning, the keograms were extensively used for studies of the auroral phenomenon in high latitudes. Afterwards, several areas began to use this technique including aeronomy done with optical probes.

In general, keograms are generated by extracting columns (south-north axis) and rows (west-east axe) from geographically mapped nightglow image data. The technique of keogram construction is ilustrated in Fig. 1. This method requires pre-processing of raw images prior any further analysis. The work of [19] describes in detail the pre-processing procedure that involves spatial calibration, star removal, geographic projection, re-gridding, and flat fielding of each image used in this study.

Here, the most important application of the keograms is related with clear signatures of plasma bubbles in nightglow images. It is possible to calculate the mean zonal drift velocity of a given event (such as addressed in the next section) as well as its horizontal extension and duration. In addition, further information can be easily taken from the keogram images such as the initial and final observation time, gaps in the data acquisition during the night due to either technical problems or unfavorable weather conditions (cloud cover or sources of light noise), etc.

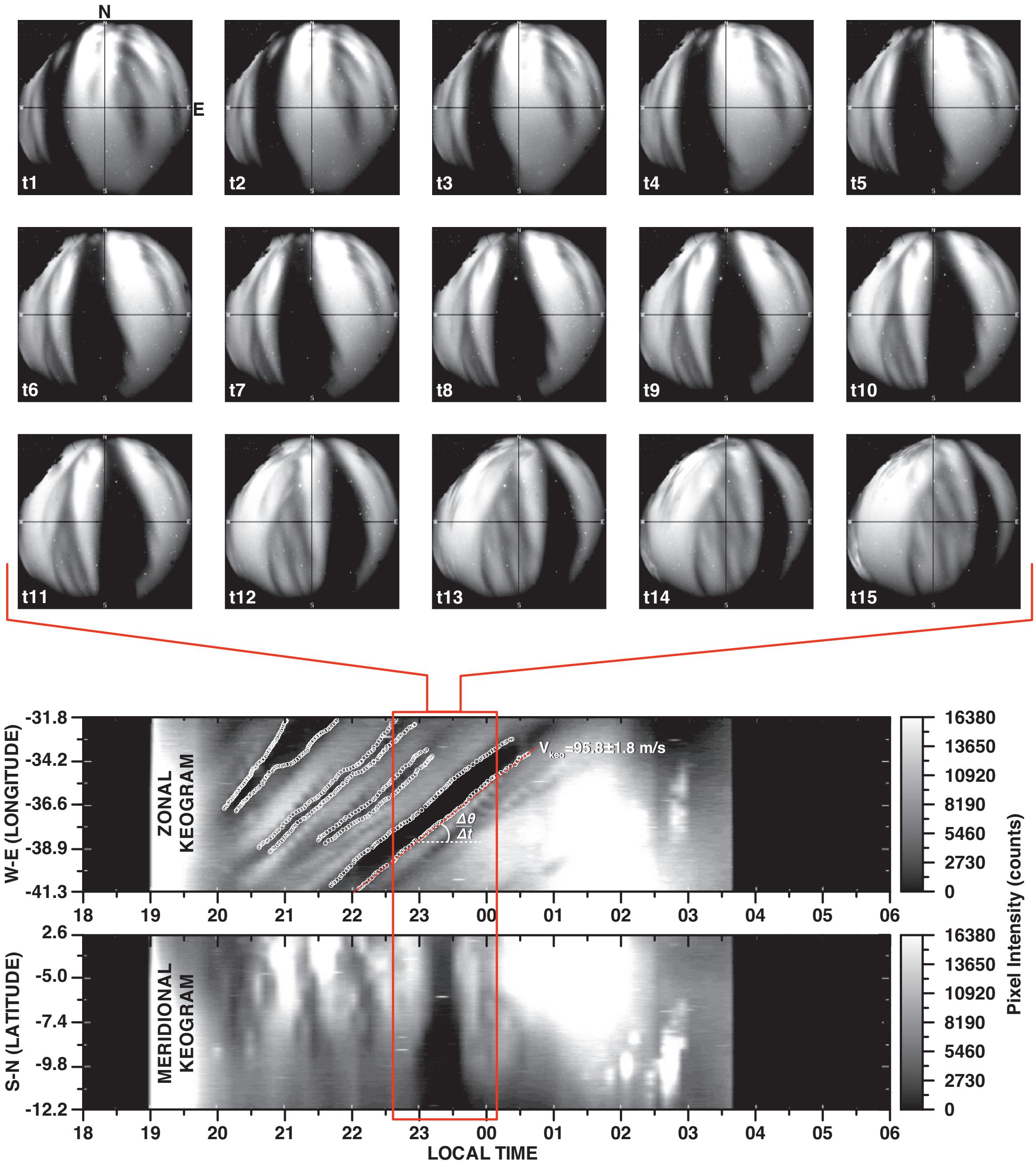

Figure 1. Illustration of how to built and derive the zonal drift velocity of a plasma bubbles from keogram images.

Peer-reviewed version available at Atmosphere 2020, 11, 69; doi:10.3390/atmos11010069

Bubble signatures in the meridional keogram exhibit a wide dark region lying along of vertical axis. The bubble structure is inverted in this frame because the frontal portion of the bubble crosses earlier the center column of the original image. In zonal keograms, the signature appears as a tilted dark region relative to the temporal axis of the image. The mean zonal drift velocity of the bubble can be computed from the zonal keogram by estimating the inclination angle between the dark structure and the temporal axis.

The inclination angle and the mean velocity of a specific plasma bubble event are related by the expression

$$v = \alpha \frac{\Delta\theta}{\Delta t},$$

where $\Delta\theta$ represents the longitude interval covered by the bubble structure in a given time interval Δt. The parameter α in this equation is an scale factor to convert the zonal drift velocity into proper physical units as follows. Raw airglow images are calibrated spatially by stellar coordinate mapping, and the spatial resolution ds of each pixel is known as well as the pixel angular resolution $d\theta$. Also, the total latitude (longitude) angle covered by all-sky images at 250 km of altitude is known for our stations from geometrical modeling [19]. Thus, the parameter α can be defined to convert the zonal drift velocity from longitude per hour ($\Delta\theta/\Delta t$) to ms^{-1}.

We calculated the mean inclination angle through a linear fitting algorithm of manually specified pixels (white circles in Fig. 1) along the bubble structure. An analysis script created to generate keograms allows to select pixels inside the tilted dark region that represents a given bubble event. The coordinates of the selected pixels (longitude, time) are stored and used as an input in the linear fitting procedure. The program calculates the best fit of the selected points, traces a straight line in the zonal keogram, and show the slope of the linear fit as presented in Fig. 1 for the entire bubble structure representing the velocity of the whole event structure. The slope of the line is the averaged rate $\Delta\theta/\Delta t$. The mean zonal drift velocity of the event is obtained by multiplying the average slope by the scale parameter α. In addition, we also use the same methodology with a 30-minutes running average of the selected points to obtain the instant zonal drift velocity of the bubble structure throughout the events duration.

3. Results

The first analysis is carried out by taking the mean zonal drift velocity of each bubble event in our dataset. As showed in the Fig. 2a, the mean zonal drift velocity decreases with local time for both CA and CP stations. A decreasing rate of $\sim$10 ms^{-1}/h was found on the linear fit of the observed zonal drift velocities. The histogram of the distribution of velocities is in Fig. 2b. The center of the distribution is in the 100 m/s bin for both sites, which are both skewed to the right.

We have also compared the keogram method presented here against the mosaic method developed by [1]. We have used the exact same data set of plasma bubble events for the comparison. We refer by v_{mosaic} the bubble zonal drift velocity calculated from the mosaic method, and by v_{keo} the zonal drift velocity estimated with the keogram method.

Fig. 3a shows a correlative analysis for the velocities calculated by the two methods. The correlation coefficient between v_{mosaic} and v_{keo} is 0.85 (R^2=0.7). The uncertainty of linear fitting coefficients is also presented in the Fig. 3 by the 95% bounds (grey dotted lines). The uncertainties are relatively small compared to the magnitude each coefficient, showing that the methods are in good statistical agreement for the estimated zonal drift velocities.

The distribution of the residuals of $v_{mosaic} - v_{keo}$ is showed in Fig. 3b. The mean value of the normal distribution for CA is 4.4 ms^{-1} and the standard deviation is 16.4 ms^{-1}. For CP, the mean is 1.2 ms^{-1} and the standard deviation is 14.2 ms^{-1}.

We obtain the instant zonal drift velocity of the bubble structure throughout the event duration by doing a 30-minutes running average of the selected pixels represented by the white circles in Fig. 1 (bottom panel), allowing to estimate the instant velocity every 30-minutes intervals. It is shown

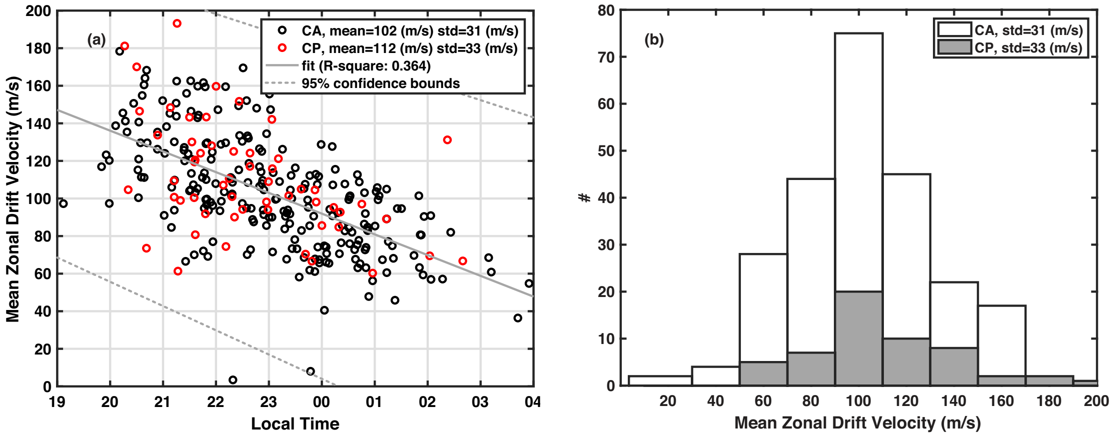

Figure 2. (a) Mean zonal drift velocities of plasma bubbles in Cariri (black) and Cachoeira Paulista (red) as function of the local time. A linear fit (gray line) depicts that smaller velocities occur in later hours of the observation period. (b) Histogram of mean zonal drift velocities distribution for Cariri (white blocks) and Cachoeira (gray blocks).

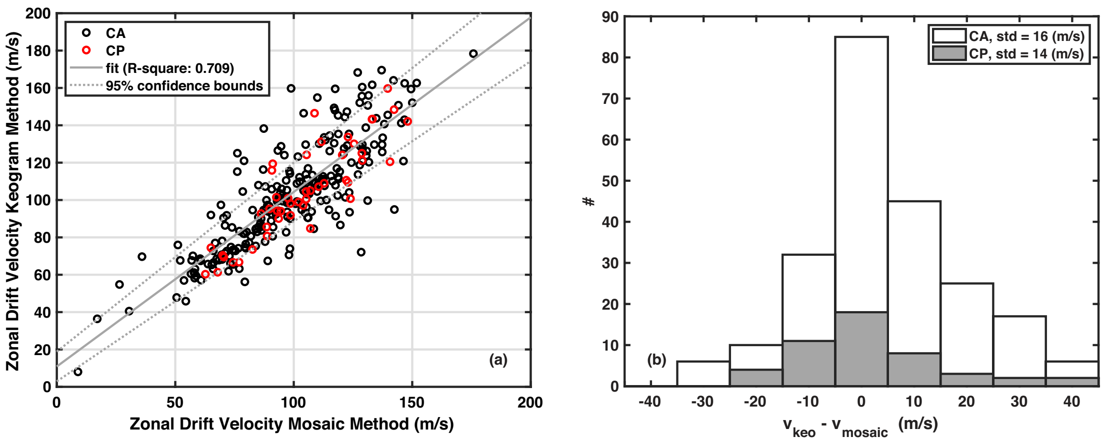

Figure 3. (a) Correlative analysis for zonal drift velocities obtained via the mosaic method against the keogram method. Back circles represent Cariri events, while red circles represent Cachoeira Paulista events. (b) Histogram of the difference between velocities computed via the mosaic method (white blocks) against the keogram method (gray blocks).

Peer-reviewed version available at Atmosphere 2020, 11, 69; doi:10.3390/atmos11010069

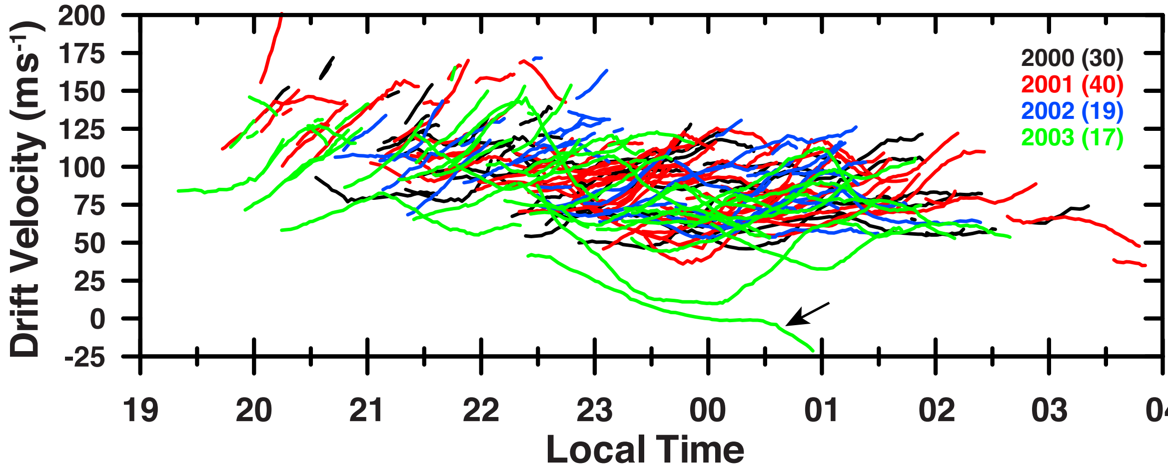

Figure 4. Instant zonal drift velocities for plasma bubbles in Cariri from 2000–2003 as function of local time.

here only the derivation carried out for CA station because it has a higher density of events detected over the years. the result is in Fig. 4. Each color represents a separated year of observation, while the numeral in parenthesis is the number of events observed during the year. Observe that a continuous line of a given color shows how the drift of the plasma bubble varies along its physical structure. remarkably, some events show positive drift velocity earlier, then changes to negative after some time, as the example pointed out by the black arrow in Fig. 4.

4. Discussion

4.1. Mean Zonal Drift Velocity × Local Time

We have showed that the mean zonal drift velocity decreases with local time. A decreasing rate of the drift velocity is of $\sim$10 ms^{-1}/h for both CA and CP stations. This rate does not mean that bubbles decelerate as they move zonally, but indicates that, if observed in later hours, bubbles are more likely to present slower drift velocities.

[13] found similar results at the low station of Cachoeira Paulista, Brazil. They calculated the decreasing rate of the mean zonal drifts of the bubbles ranging from -14.5 ms^{-1} to $\sim$8.5 ms^{-1}, depending on the season and solar activity. The decreasing of the drift velocity of bubble events represents the influence of the neutral wind on the bubble dynamics. The polarization electric field that drives the F region nocturnal zonal drift is very intense after sunset and decreases with time because of the reduced neutral wind velocity, causing the ionospheric plasma to drag along by vertical electric fields generated by the zonal wind.

The comparison of the keogram method against the mosaic method developed by [1] shows somewhat large standard deviations for the normal distribution of $v_{mosaic} - v_{keo}$ in Fig. 3b. This points out to a slight disagreement between the two methods. For instance, while $\sim$68% of the events present relative difference of less than $\sim$15 ms^{-1}, more than $\sim$30% of them has a residual larger than 15 ms^{-1} for the estimated zonal drift velocity. Considering that the overall mean of observed zonal drift velocities is $\sim$100 ms^{-1}, the relative error would be larger than 15%. That points out that one third of the time the results from these two methods will differ by >15 ms^{-1}.

4.2. Zonal Drift Velocity × Local Time × Geographical Longitude

From the instant zonal drift velocity in Fig. 4, we can show how the bubble drift velocity varies with local time and latitude (Fig. 4). This is possible because the keogram method allows for the mapping of the bubble velocity along the longitudinal structure of the event. For example, the event

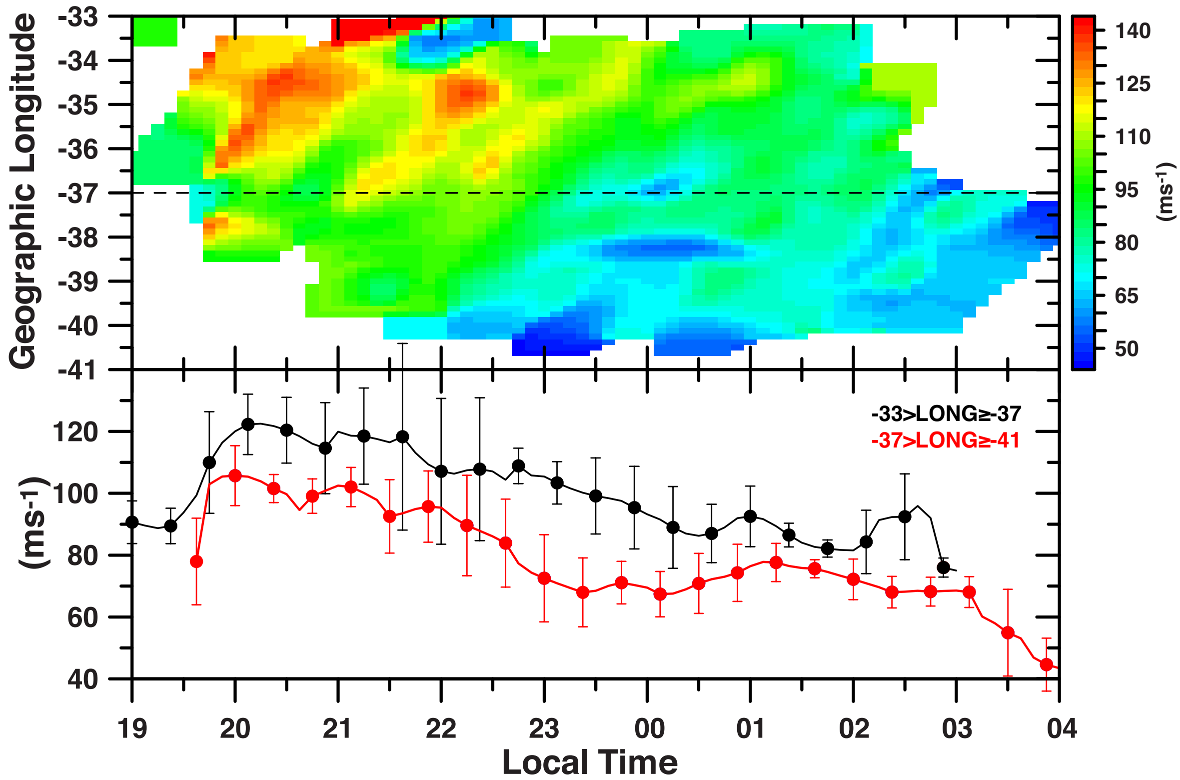

Figure 5. (Top) Zonal drift velocity versus local time and geographic longitude for the Cariri observatory. (Bottom) Drift velocity versus time along distinct longitude ranges.

starting at 20 LT in Fig. 2 shows that the tilt structure from 20 LT changes after 21 LT. To built the top panel of Fig. 5, we have used all the points along the bubble structures collected for each event. Based on that, we see in the bottom panel of Fig. 5 that larger zonal drift velocities for appear in the west-most side of zonal keograms (-37° to -33° longitude). Also, in this latitude range between 21-23 LT, the zonal drift velocities are larger. This may be associated with the neutral wind behavior and a locally disturbed ionospheric dynamo.

5. Summary and Conclusion

We presented in this work a new method to analyze ionosphere plasma bubbles events and calculated their mean zonal drift velocities using keograms images. The data set comprises images of OI6300 nightglow emission obtained in Cariri (7.4°S, 36.5°W), an equatorial site, and Cachoeira Paulista (22.7°S, 45°W), a mid latitude site. Both stations are located over the Brazilian sector. Images from CA were taken from 2000 to 2003, while from from 1998 to 2000 in CP. The main findings of this work are:

- In general, mean zonal drift velocities of plasma bubbles decrease throughout the night. Larger velocity events travel at ~150 ms^{-1} (usually occurring during earlier hours of the observing period), while slower events move at ~60 ms^{-1} (occurring late in the observation period). The decreasing rate is ~10 ms^{-1}/h.
- Typically, faster plasma bubbles occur from 20 LT to 23 LT in the west-most region of the zonal keograms in a longitude range of -37° to -33°.
- Our keogram technique compares favorably with the mosaic method [1]. A Gaussian curve fits well the velocity differences distribution of $v_{mosaic} - v_{keo}$. The standard deviation of the residuals distribution is large (~15ms^{-1}). Moreover, >30% of the residuals of $v_{mosaic} - v_{keo}$ have values larger than 15 ms^{-1}, which points out to possible refining of the methods.

Author Contributions: Formal analysis, F.V.; Investigation, F.V. and C.B.; Methodology, F.V.; Resources, D.G.; Writing – original draft, F.V.; Writing – review editing, F.V. and C.B. and P.T.

Funding: This research received no external funding by CNPq grant number 04/07695-5 and National Science Foundation under 1-NSF AGS Grant 17-59573 and 2-NSF AGS Grant 19-03336.

Acknowledgments: We are grateful to Capes, and FAPESP, the Brazilian Financial Agencies, that gave support to this work in several ways. The Arecibo Observatory is a facility of the National Science Foundation operated under cooperative agreement by the University of Central Florida (UCF) in alliance with Yang Enterprises, Inc., and Universidad Ana G. Mendez (UAGM).

Conflicts of Interest: The authors declare no conflict of interest.

References

1. Arruda, D.C.S. Study of the nocturnal ionosphere F-layer zonal drifts over the Brazilian region. PhD thesis, Instituto Nacional de Pesquisas Espaciais (INPE), São José dos Campos, 2005.
2. Abdu, M.A.; Muralikrishna, P.; Batista, I.S.; Sobral, J.H.A. Rocket observation of equatorial plasma bubbles over Natal, Brazil, using a high-frequency capacitance probe. *Journal of Geophysical Research: Space Physics* **1991**, *96*, 7689–7695, [https://agupubs.onlinelibrary.wiley.com/doi/pdf/10.1029/90JA02384]. doi:10.1029/90JA02384.
3. Abdu, M. Outstanding problems in the equatorial ionosphere–thermosphere electrodynamics relevant to spread F. *Journal of Atmospheric and Solar-Terrestrial Physics* **2001**, *63*, 869 – 884.
4. Dos Santos Prol, F.; Hernández-Pajares, M.; Tadeu de Assis Honorato Muella, M.; De Oliveira Camargo, P. Tomographic Imaging of Ionospheric Plasma Bubbles Based on GNSS and Radio Occultation Measurements. *Remote Sensing* **2018**, *10*.
5. Silva, R.P.; Souza, J.R.; Sobral, J.H.A.; Denardini, C.M.; Borba, G.L.; Santos, M.A.F. Ionospheric Plasma Bubble Zonal Drift Derived From Total Electron Content Measurements. *Radio Science* **2019**, *54*, 580–589.
6. Abalde, J.R.; Fagundes, P.R.; Bittencourt, J.A.; Sahai, Y. Observations of equatorial F region plasma bubbles using simultaneous OI 777.4 nm and OI 630.0 nm imaging: New results. *Journal of Geophysical Research: Space Physics* **2001**, *106*, 30331–30336.
7. Abalde, J.R.; Fagundes, P.R.; Sahai, Y.; Pillat, V.G.; Pimenta, A.A.; Bittencourt, J.A. Height-resolved ionospheric drifts at low latitudes from simultaneous OI 777.4 nm and OI 630.0 nm imaging observations. *Journal of Geophysical Research: Space Physics* **2004**, *109*, [https://agupubs.onlinelibrary.wiley.com/doi/pdf/10.1029/2004JA010560]. doi:10.1029/2004JA010560.
8. Arruda, D.C.; Sobral, J.; Abdu, M.; Castilho, V.M.; Takahashi, H.; Medeiros, A.; Buriti, R. Theoretical and experimental zonal drift velocities of the ionospheric plasma bubbles over the Brazilian region. *Advances in Space Research* **2006**, *38*, 2610 – 2614. Middle and Upper Atmospheres, Active Experiments, and Dusty Plasmas, doi:https://doi.org/10.1016/j.asr.2006.05.015.
9. Sobral, J.; Abdu, M.; Sahai, Y. Equatorial plasma bubble eastward velocity characteristics from scanning airglow photometer measurements over Cachoeira Paulista. *Journal of Atmospheric and Terrestrial Physics* **1985**, *47*, 895 – 900. doi:https://doi.org/10.1016/0021-9169(85)90064-9.
10. Sobral, J.H.A.; Abdu, M.A. Latitudinal gradient in the plasma bubble zonal velocities as observed by scanning 630-nm airglow measurements. *Journal of Geophysical Research: Space Physics* **1990**, *95*, 8253–8257, [https://agupubs.onlinelibrary.wiley.com/doi/pdf/10.1029/JA095iA06p08253]. doi:10.1029/JA095iA06p08253.
11. Pimenta, A.; Bittencourt, J.; Fagundes, P.; Sahai, Y.; Buriti, R.; Takahashi, H.; Taylor, M. Ionospheric plasma bubble zonal drifts over the tropical region: a study using OI 630nm emission all-sky images. *Journal of Atmospheric and Solar-Terrestrial Physics* **2003**, *65*, 1117 – 1126.
12. Takahashi, H.; Taylor, M.J.; Pautet, P.D.; Medeiros, A.F.; Gobbi, D.; Wrasse, C.M.; Fechine, J.; Abdu, M.A.; Batista, I.S.; Paula, E.; Sobral, J.H.A.; Arruda, D.; Vadas, S.L.; Sabbas, F.S.; Fritts, D.C. Simultaneous observation of ionospheric plasma bubbles and mesospheric gravity waves during the SpreadFEx Campaign. *Annales Geophysicae* **2009**, *27*, 1477–1487. doi:10.5194/angeo-27-1477-2009.
13. Terra, P.M.; Sobral, J.H.A.; Abdu, M.A.; Souza, J.R.; Takahashi, H. Plasma bubble zonal velocity variations with solar activity in the Brazilian region. *Annales Geophysicae* **2004**, *22*, 3123–3128. doi:10.5194/angeo-22-3123-2004.

14. Sobral, J.; Abdu, M.; Takahashi, H.; Taylor, M.; de Paula, E.; Zamlutti, C.; de Aquino, M.; Borba, G. Ionospheric plasma bubble climatology over Brazil based on 22 years (1977–1998) of 630nm airglow observations. *Journal of Atmospheric and Solar-Terrestrial Physics* **2002**, *64*, 1517 – 1524.
15. Taylor, M.J.; Eccles, J.V.; LaBelle, J.; Sobral, J.H.A. High resolution OI (630 nm) image measurements of F-region depletion drifts during the Guará Campaign. *Geophysical Research Letters* **1997**, *24*, 1699–1702, [https://agupubs.onlinelibrary.wiley.com/doi/pdf/10.1029/97GL01207]. doi:10.1029/97GL01207.
16. Takahashi, H.; Wrasse, C.M.; Figueiredo, C.A.O.B.; Barros, D.; Abdu, M.A.; Otsuka, Y.; Shiokawa, K. Equatorial plasma bubble seeding by MSTIDs in the ionosphere. *Progress in Earth and Planetary Science* **2018**, *5*, 32.
17. Vargas, F. Travelling Ionosphere Disturbance Signatures on Ground-Based Observations of the $O(^1D)$ Nightglow Inferred from 1D Modeling. *Journal of Geophysical Research: Space Physics - Accepted Manuscript* **2019**, -, –.
18. Medeiros, A.; Buriti, R.; Machado, E.; Takahashi, H.; Batista, P.; Gobbi, D.; Taylor, M. Comparison of gravity wave activity observed by airglow imaging at two different latitudes in Brazil. *Journal of Atmospheric and Solar-Terrestrial Physics* **2004**, *66*, 647 – 654. Dynamics and Chemistry of the MLT Region - PSMOS 2002 International Symposium, doi:https://doi.org/10.1016/j.jastp.2004.01.016.
19. Garcia, F.J.; Taylor, M.J.; Kelley, M.C. Two-dimensional spectral analysis of mesospheric airglow image data. *Appl. Opt.* **1997**, *36*, 7374–7385. doi:10.1364/AO.36.007374.